The Application of Competitive Hopfield Neural Network to Medical Image Segmentation

Kuo-Sheng Cheng,* *Member, IEEE*, Jzau-Sheng Lin, and Chi-Wu Mao

***Abstract*—In this paper, a parallel and unsupervised approach using the competitive Hopfield neural network (CHNN) is proposed for medical image segmentation. It is a kind of Hopfield network which incorporates the winner-takes-all (WTA) learning mechanism. The image segmentation is conceptually formulated as a problem of pixel clustering based upon the global information of the gray level distribution. Thus, the energy function for minimization is defined as the mean of the squared distance measures of the gray levels within each class. The proposed network avoids the onerous procedure of determining values for the weighting factors in the energy function. In addition, its training scheme enables the network to learn rapidly and effectively. For an image of n gray levels and c interesting objects, the proposed CHNN would consist of n by c neurons and be independent of the image size. In both simulation studies and practical medical image segmentation, the CHNN method shows promising results in comparison with two well-known methods: the hard and the fuzzy c-means (FCM)methods.**

I. Introduction

In medical image visualization and analysis, segmentation is an indispensable step in the processing. Due to the characteristics of the imaging modalities for use in clinics, the produced image reveals different tissue properties for diagnosis. In addition, the anatomical structure is complicated and varied. Therefore, segmentation becomes a difficult but important problem in biomedical applications. It is a technique for partitioning the image into meaningful subregions or objects with the same attribution, and usually is image and application dependent. A number of algorithms based upon approaches such as histogram analysis, region growing, edge detection, and pixel classification have been proposed in the past [1]–[5]. Generally speaking, these methods make use of the local information (i.e., the gray-level values of the neighboring pixels) and/or the global information (i.e., the overall gray-level distribution of the image) for image segmentation. Some algorithms using the neural network approach have also been investigated in the image segmentation problems [11], [23].

Manuscript received December 13, 1994; revised April 22, 1996. This work was supported in part by the National Science Council, ROC, under Grant #NSC83-0412-B006-040-M08, and the Medical Imaging Research Group, National Cheng Kung University. The Associate Editor responsible for coordinating the review of this paper and recommending its publication was C. Roux. *Asterisk indicates corresponding author.*

*K.-S. Cheng is with the Institute of Biomedical Engineering, National Cheng Kung University, Tainan 70101, Taiwan, ROC (e-mail: kscheng@decl.bme.ncku.edu.tw).

J.-S. Lin and C.-W. Mao are with the Institute of Electrical Engineering, National Cheng Kung University, Tainan 70101, Taiwan, ROC.

Publisher Item Identifier S 0278-0062(96)05750-3.

Recently, a method based upon two four-layer neural networks was applied to segment the magnetic resonance (MR) images of the brain into the white, gray, and other tissues [6]. This approach basically incorporated both the information obtained from the MR tissue signature and the anatomical structure. In this method, one neural network was designed for the sequence reconstructor subsystem, and the other was employed for classifying the pixels of MR image into proper regions. A three-dimensional (3-D) constraint satisfaction neural network for image segmentation was presented by Lin *et al.* [7]. In it, the spatial constraints were added for merging the regions. The segmentation of MR images using the probabilistic neural network was investigated by Morrison *et al.* [8], and the segmentation of MR brain images using mean field simulated annealing was discussed by Snyder *et al.* [9]. Dhawan and Arata presented a self-organizing feature map algorithm for the segmentation of medical image with competitive learning [10]. Their network was composed of two-dimensional (2-D) input (gray-level image) and output (segmented feature map) layers for combining the local contrast as well as the global gray-level distribution information to find out the desired regions. A comparison of the methods for a supervised multilayer feedforward neural network, a dynamic multilayer perceptron trained with cascade correlation, and a fuzzy c-means unsupervised clustering in segmenting MR brain images into seven classes was presented by Hall *et al.* [11].

Image segmentation may be considered as a clustering process in which the pixels are classified into the attributed regions based upon their gray-level values and spatial connectivity. In this paper, a new image segmentation method using a competitive Hopfield neural network (CHNN) based upon the global gray-level distribution is proposed. The problem of image segmentation is regarded as a minimization of the cost function, which is defined as the mean value of distance measures between the gray-level values and the member of classes. The structure of this network is implemented as a 2-D array with the columns representing the number of classes and the rows representing the gray levels. It is modified from the original Hopfield network to incorporate a competitive i.e., winner-takes-all (WTA) learning mechanism. Therefore, the energy function may be fast to converge, and then to produce a satisfactory resulting image. In the simulation study, the CHNN is demonstrated to have the capability for image segmentation and robustness to the noise. In addition, the CHNN method is also compared with both the hard c-means (HCM) and fuzzy c-means (FCM) methods in the practical applications of medical image segmentation.

The remainder of this paper is organized as follows. Section II reviews the HCM and FCM algorithms. In Section III, the image segmentation using a CHNN is described. The advantages of using a WTA learning in Hopfield network are also discussed. Section IV discusses the convergence of the CHNN on the mathematical derivations. Some experimental results, and the performances comparison of the HCM, FCM algorithms and the proposed method are given in Section V. Finally some conclusions are made in Section VI.

II. Hard and Fuzzy C-Means for Image Segmentation

For the sake of completeness, two frequently used image segmentation methods i.e., hard c-means and fuzzy c-means, are described briefly as follows in comparison with the proposed CHNN method.

A. The Hard C-Means Algorithm (HCM)

In HCM algorithm, the number of classes in the image is usually known *a priori*. If not, at least a rough idea of the number and the locations of the clusters should be available beforehand.

Let $G = \{g_1, g_2, \cdots, g_n\}$ be a set of any finite gray levels of n, the integer $c(2 \le c < n)$ be the number of classes, where c is the total number of classes, and M be the matrix of n by c. The matrix $V = [v_{x,i}] \in M_{n,c}$ is called a hard c-partition if it satisfies the following conditions:

$$v_{x,i} \in \{0, 1\}, \quad \text{for} \quad 1 \le x \le n, \quad 1 \le i \le c \tag{1}$$

$$\sum_{i=1}^{c} v_{x,i} = 1, \quad \text{for} \quad 1 \le x \le n \tag{2}$$

$$0 < \sum_{x=1}^{n} v_{x,i} < n, \quad \text{for} \quad 1 \le i \le c \tag{3}$$

$$\sum_{x=1}^{n} \sum_{i=1}^{c} v_{x,i} = n. \tag{4}$$

The basic form of algorithm described in many articles [12]–[15] is summarized as follows.

Algorithm of HCM:

Step 1) Arbitrarily choose the initial class centers z_i of the gray levels with $1 \le i \le c$.

Step 2) Find the pixel number h_x at gray level g_x from the histogram of an image.

Step 3) Assign every gray level to the attributive class based upon the minimum square Euclidean distance measure between the gray levels and the class centers.

Step 4) Update the class centers as follows:

$$z_i = \frac{\sum_x h_x g_x v_{x,i}}{\sum_x h_x v_{x,i}}.$$

Step 5) Check the convergence behavior. If the changes of the class centers are below some specified threshold value, then stop; otherwise, go to Step 3).

It is easily seen that the class centers would be sequentially updated, and also that the performance of this HCM algorithm would be affected both by the initially chosen number of class centers and by the gray levels.

B. The Fuzzy C-Means Algorithm (FCM)

Fuzzy theory has been applied in a variety of fields, such as industrial control, computer vision, linear programming, and even drug infusion systems. Hall *et al.* [11] extensively investigated the performance comparisons between two fuzzy clustering techniques (the FCM method and an approximation of it), a neural network-based procedure, and a HCM clustering method for medical image segmentation. Brandt *et al.* [16] used an FCM approach to estimate the volumes of cerebrospinal fluid, white and gray matters from the transaxial MR images of the brain.

In the HCM method, a pixel only belongs to one class. Whereas in the FCM method, every pixel belongs to all classes with different degrees of the membership functions. The procedure of the FCM algorithm is summarized in the following steps [11]–[13], [16], [17].

Algorithm of FCM:

Step 1) Arbitrarily choose the initial class centers z_i of the gray levels with $1 \le i \le c$, where c is the total number of classes.

Step 2) Find the pixel number h_x at gray level g_x from the histogram of an image.

Step 3) Compute the square Euclidean distance measure between the gray levels g_x and the class center z_i for all classes as follows:

$$d_{x,i}^2 = \| g_x - z_i \|^2, \quad \text{for} \quad 1 \le x \le n, \quad 1 \le i \le c.$$

Step 4) Calculate the membership matrix U given as

$$u_{x,i} = \frac{\left[\frac{1}{(d_{x,i})^2}\right]^{1/(m-1)}}{\sum_{i=1}^{c} \left[\frac{1}{(d_{x,i})^2}\right]^{1/(m-1)}}, \quad \text{for} \quad g_x \ne z_x$$

and

$$u_{x,i} = \begin{cases} 1, & \text{if } x = i, \\ 0, & \text{otherwise.} \end{cases}$$

Step 5) Update the class centers as

$$z_i = \frac{1}{\sum_{x=1}^{n} (u_{x,i})^m h_x} \sum_{x=1}^{n} (u_{x,i})^m g_x h_x.$$

Step 6) Check $\triangle = \max[|U^{(t+1)} - U^{(t)}|]$. If $\triangle > \varepsilon$, then go to Step 4). Otherwise, stop.

The initial value m, called the exponential weight (or the fuzzification parameter), is set to be two, and it will alleviate the noise effect when computing the class centers. The larger the value of m (greater than one) is, the more the sensitivity of the noise will be.

In the following section, the competitive Hopfield neural network proposed for the medical image segmentation will be described in detail.

III. The Competitive Hopfield Neural Network

In the constraint satisfaction neural network proposed by Lin *et al.* [7], each pixel in an L × L image would be considered as an object to be assigned to one of M labels. Thus, it consists of L × L × M neurons which can be conceived as a 3-D array for the image segmentation problem. The number of neurons are dependent on image size. The larger the image size is, the more the neurons are needed. Thus, the neural network becomes very complicated in computation.

In this paper, the global gray levels distribution rather than the spatial connectivity information of the medical images is employed for the image segmentation. In [18], Chung *et al.* proposed the competitive Hopfield neural network for polygonal approximation. Here, the CHNN is modified and extended for application to medical image segmentation.

For a 2-D image with the number of gray levels n and a set of predefined subregions c, then the CHNN consists of n by c neurons as a 2-D array. Therefore, the number of neurons is independent of the image size. The Hopfield neural network, with its features of simple architecture and potential for parallel implementation, has been applied in many fields [18]–[21]. The network used in this study is designed to be based upon a Lyapunov energy function. Hence, the Hopfield neural network is a good technique for solving the optimization problem. In this section, it is shown that the image segmentation problem can be mapped onto a Hopfield neural network so that the cost function serves as the energy function of the network. The iteratively updated synaptic weights between the neuronal interconnections will gradually force the network to converge to a stable state as its energy function is minimized. The distance measure between the pairs of gray levels in a given picture is used for pixel classification. However, the number of classes needs to be specified in advance. The clustering based image segmentation method for this proposed CHNN can be described as follows.

Let the brightness of a given image be represented by n gray levels. The number of pixels at the gray-level x is denoted by h_x and the total number of pixels will be equal to $\sum_{x=1}^{n} h_x$ And, $d(x, y)$ indicating the square of the Euclidean distance measure between the gray-level pairs g_x and g_y is defined as

$$\begin{aligned} d_{x,y} &= d(g_x, g_y) \\ &= (g_x - g_y)^2. \end{aligned} \tag{5}$$

For a set of gray-level values, $G = \{g_1, g_2, \cdots, g_n\}$, the set of all the square distance measure DIS $= \{d_{x,y}\}$ with $x = 1, 2, \cdots, n$, and $y = 1, 2, \cdots, n$, may then be obtained according to (5). It should be noted that the square distance measure is symmetric i.e., $d_{x,y} = d_{y,x}$.

Based on this distance measure for the gray levels, a new image segmentation technique using the competitive Hopfield neural network has been developed. For the given numbers of gray levels and their classes, the proposed method is to assign every gray level to the appropriate class such that the mean value of the distance between gray-level values and the center of a certain class is minimum in an image.

This network consists of n by c neurons which are mutually interconnected. All the parameters are defined as (1)–(4). Let $V_{x,i}$ denote the binary state of the (x, i)th neuron and $W_{x,i;y,j}$ be the interconnection weight between the neuron (x, i) and the neuron (y, j). A neuron (x, i) in this network would receive the inputs weighted by $W_{x,i;y,j}$ from every other neuron (y, j), and also an additional bias $I_{x,i}$. The total input to the neuron (x, i) may be calculated as

$$Net_{x,i} = \sum_{y=1}^{n} \sum_{j=1}^{c} W_{x,i;y,j} V_{y,j} + I_{x,i} \tag{6}$$

and the Lyapunov energy function of the 2-D Hopfield network is given as follows:

$$\begin{aligned} E = &-\tfrac{1}{2} \sum_{x=1}^{n} \sum_{y=1}^{n} \sum_{i=1}^{c} \sum_{j=1}^{c} V_{x,i} W_{x,i;y,j} V_{y,j} \\ &- \sum_{x=1}^{n} \sum_{i=1}^{c} I_{x,i} V_{x,i}. \end{aligned} \tag{7}$$

The columns of the Hopfield network represent the given classes, and the rows represent the gray levels in an image. The network will approach to a stable state when the Lyapunov energy function is minimized. For example, a neuron $V_{x,i}$ in a firing state (binary state = 1) indicates that the gray level g_x belongs to class i. The objective function for describing the pixel classification of the image segmentation based upon the mean value of the square Euclidean distance measure between the gray levels to the members of classes is defined as

$$\begin{aligned} E = &\frac{A}{2} \sum_{x=1}^{n} \sum_{y=1}^{n} \sum_{i=1}^{c} \frac{1}{\sum_{y=1}^{n} h_y V_{y,i}} V_{x,i} d_{x,y} h_y V_{y,i} \\ &+ \frac{B}{2} \sum_{x=1}^{n} \sum_{i=1}^{c} \sum_{j=1}^{c} V_{x,i} V_{x,j} \\ &+ \frac{C}{2} \left[\left(\sum_{x=1}^{n} \sum_{i=1}^{c} V_{x,i} \right) - n \right]^2. \end{aligned} \tag{8}$$

The first summation term in the right-hand side is the total mean square of the distance measures. The second term, the energy form of (2), attempts to ensure that no gray level g_x would simultaneously appear in two or more classes in the segmented image. The third term, being the energy form of (4), is added to make sure the total classes not greater than the total gray levels n. It is noted that the last two penalty terms are used as the constraints for the image segmentation, while the first term is employed for delineating the mean square distance measures between the gray levels and the centers of the classes. However, as has been pointed out in reference [18], the finally obtained solution is very sensitive to the values of these weighting factors A, B, and C. The task of searching the optimal values for these weighting factors would be time-consuming and laborious.

In this paper, a CHNN is proposed for solving the above mentioned problem. The competitive learning rule, WTA, is used for updating the weightings among the neurons. Therefore, the penalty terms may be handled in an efficient and explicit manner. Only one of the neurons in each row which

receives the maximum input would be the winner neuron with its output being set at one. The outputs of all the other neurons on the same row would then be set at zero. In other words, the input–output function for the xth row is given as

$$V_{x,i} = \begin{cases} 1, & \text{if } Net_{x,i} = \max\{Net_{x,1}, Net_{x,2}, \cdots Net_{x,c}\}, \\ 0, & \text{otherwise.} \end{cases} \tag{9}$$

The WTA learning rule would also guarantee that no two gray levels g_x and g_y would be assigned to the same class. In addition, it ensures that every gray level of an image will be classified into a prior known class number. The energy function of the modified Hopfield neural network should converge to a minimum value. Thus, the objective energy function of the CHNN may be simplified as follows:

$$E = \sum_{x=1}^{n}\sum_{y=1}^{n}\sum_{i=1}^{c} \frac{1}{\sum_{y=1}^{n} h_y V_{y,i}} V_{x,i} d_{x,y} h_y V_{y,i}. \tag{10}$$

There are no more penalty terms in (10), and only one term is needed to be minimized. Hence, the problem of determining the optimal values of the weighting factors will be avoided. Comparing (10) with the Lyapunov function of (7) for the Hopfield network, the synaptic interconnection weights and the bias input may be obtained as

$$W_{x,i;y,j} = -\frac{1}{\sum_{y=1}^{n} h_y V_{y,i}} d_{x,y} h_y \tag{11}$$

and

$$I_{x,i} = 0 \tag{12}$$

respectively. Substituting (11) into (6), the total inputs to the neuron (x, i) may be represented as

$$Net_{x,i} = -\frac{1}{\sum_{y=1}^{n} h_y V_{y,i}} \sum_{y=1}^{n} d_{x,y} h_y V_{y,i}. \tag{13}$$

As seen from the energy function, the proposed CHNN is conceived as the process of the pixel classification which minimizes the objective function in a parallel structure. When the number of classes c is given, the proposed method can be used to classify the n gray levels into their attributed classes. The topology of the CHNN is depicted in Fig. 1, and its algorithm is summarized as follows.

Algorithm of CHNN:

Step 1) Input the gray levels of n, $G = \{g_1, g_2, \cdots, g_n\}$ and the number of classes of an image.

Step 2) Compute the distance measure DIS $= \{d_{x,y}\}$ and the histogram $\{h_y\}$, where $x = 1, 2, \cdots, n$, and $y = 1, 2, \cdots, n$.

Step 3) Set the initial number of the neurons to be n. Every class contains at least one gray level.

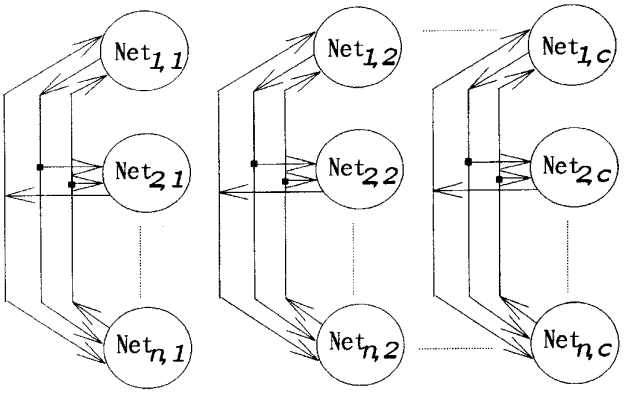

Fig. 1. The architecture of the proposed CHNN with n by c neurons. n is the total number of gray levels and c is the prespecified class number.

Step 4) Calculate the total input of each neuron (x, i) in a row x as

$$Net_{x,i} = -\frac{1}{\sum_{y=1}^{n} h_y V_{y,i}} \sum_{y=1}^{n} d_{x,y} h_y V_{y,i}.$$

Step 5) Apply the WTA learning scheme as shown in (9) to compute the new output value for each neuron on the row.

Step 6) Repeat Steps 4) and 5) for all rows, and count the number of neurons for the new state. If there are no changing neurons, then go to Step 7). Otherwise, go to Step 4).

Step 7) Output the final state of neurons that indicates the gray levels being assigned to the given classes.

IV. The Convergence of CHNN

The energy function of the proposed CHNN is always convergent during the network evolutions. The proof of the mathematical derivations is discussed as follows. The energy function defined for this proposed CHNN as shown below in (14) may be further broken into two terms

$$E = \sum_{x=1}^{n}\sum_{y=1}^{n}\sum_{i=1}^{c} \frac{1}{\sum_{y=1}^{n} h_y V_{y,i}} V_{x,i} d_{x,y} h_y V_{y,i}. \tag{14}$$

One contains the terms of $x = p$, and the other is the rest of the terms as shown in the following (15):

$$\begin{aligned} E &= E_p + E_o \\ &= \frac{1}{\sum_{y=1}^{n} h_y V_{y,i}} \left(\sum_{y=1}^{n}\sum_{i=1}^{c} V_{p,i} d_{p,y} h_y V_{y,i} \right. \\ &\quad \left. + \sum_{x=1;\, x\neq p}^{n}\sum_{y=1}^{n}\sum_{i=1}^{c} V_{x,i} d_{x,y} h_y V_{y,i} \right) \end{aligned} \tag{15}$$

where E_p and E_o stand for the energy of the row $x = p$ and the other rows, respectively. Thus, only the first term will be affected by the states of the row p. The WTA learning scheme guarantees that each row contains only one active neuron. Without loss of generality, it is assumed that the neuron (p, a) is the only active neuron in the pth row before updating i.e., $V_{p,a}^{(t)} = 1$ and $V_{p,i}^{(t)} = 0$ for all $i \neq a$. After updating, the neuron (p, b) is selected to be the winning node i.e., $V_{p,b}^{(t+1)} = 1$ and $V_{p,i}^{(t+1)} = 0$ for all $i \neq b$.

According to (13) and the WTA learning scheme of (9), we have

$$\sum_{y=1}^{n} \frac{1}{\sum_{y=1}^{n} h_y V_{y,b}} d_{p,y} h_y V_{y,b} = \max_{i=1,2,\cdots,c} \left\{ \sum_{y=1}^{n} \frac{-1}{\sum_{y=1}^{n} h_y V_{y,i}} d_{x,y} h_y V_{y,i} \right\}. \quad (16)$$

This implies that

$$\sum_{y=1}^{n} \frac{1}{\sum_{y=1}^{n} h_y V_{y,b}} d_{p,y} h_y V_{y,b} < \sum_{y=1}^{n} \frac{1}{\sum_{y=1}^{n} h_y V_{y,a}} d_{p,y} h_y V_{y,a}. \quad (17)$$

Thus, according to (16), the changes of the energy ($\triangle E$) of the pth row could be computed as

$$\begin{aligned} \triangle E &= E^{(t+1)} - E^{t} \\ &= \frac{1}{\sum_{y=1}^{n} h_y V_{y,b}} \sum_{y=1}^{n} V_{p,b}^{(t+1)} d_{p,y} h_y V_{y,b} \\ &\quad - \frac{1}{\sum_{y=1}^{n} h_y V_{y,a}} \sum_{y=1}^{n} V_{p,a}^{(t)} d_{p,y} h_y V_{y,a} \end{aligned} \quad (18)$$

where $V_{p,b}^{(t+1)}$ and $V_{p,a}^{(t)}$ are set to be one in (18). From (17), it is seen that $\triangle E$ for the changes of energy during the updating process is decreasing. Therefore, the convergence of the CHNN is guaranteed.

V. Simulation and Experimental Results

The performances for two frequently-used methods i.e., the HCM and FCM, and the proposed algorithm were first compared in the simulation study. The computer generated image was made up of seven overlapping ellipses. Each ellipse represents one structural area of tissue. From the periphery to the center, they were the background (BKG, gray level = 30), skin or fat (S/F, gray level = 75), gray matter (GM, gray level = 120), white matter (WM, gray level = 165), and cerebrospinal fluid (CSF, gray level = 210), respectively. The gray levels for each region were set to a constant value. In addition, the noise of uniform distribution with the gray levels ranging from $-K$ to K was then added to this simulation phantom. The noise level K for different cases was set to be 18, 20, 23, and 25, respectively. The resulting images for the simulation study are shown in Figs. 2–4. The accuracy for the three image segmentation methods described above are listed in Tables I–III. The values for the accuracy are the averaged value for ten runs with different random initial noise. From these tables, it can easily be seen that all the methods would extract the objects very accurately for the noise levels $K = 18$ and 20, respectively. For larger noise levels of $K = 23$ and 25, the proposed algorithm based upon the CHNN would be more accurate in image segmentation than the other two methods. An average accuracy about 97.3% for $K = 23$, and 91.2% for $K = 25$ may be achieved using the CHNN approach.

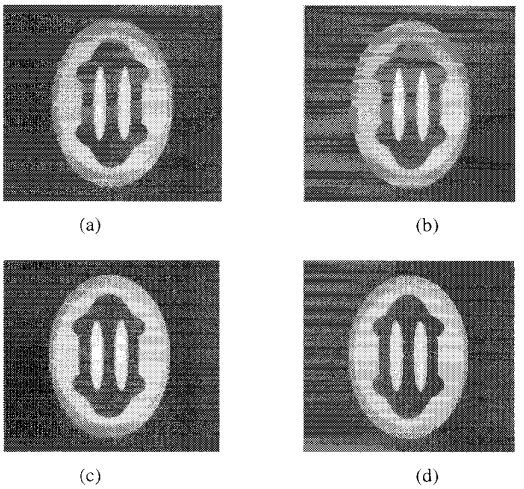

Fig. 2. The simulated image of four objects with added noise ($K = 18/20$) in (a), (b), (c), and (d) show the resulting images using the HCM, FCM, and CHNN methods, respectively.

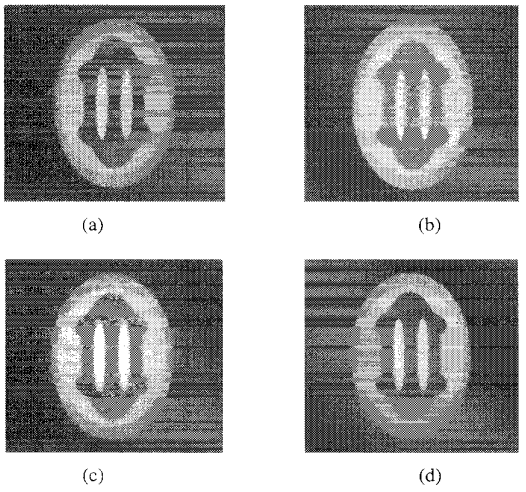

Fig. 3. The simulated image of four objects with added noise ($K = 23$) in (a), (b), (c), and (d) show the resulting images using the HCM, FCM, and CHNN methods, respectively.

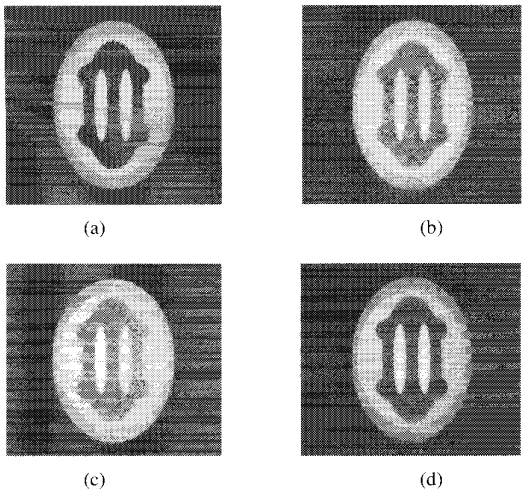

Fig. 4. The simulated image of four objects with added noise ($K = 25$) in (a), (b), (c), and (d) show the resulting images using the HCM, FCM, and CHNN methods, respectively.

TABLE I
THE SEGMENTATION PERFORMANCES FOR HCM, FCM, AND THE PROPOSED CHNN METHODS USING THE SIMULATED IMAGE WITH $K = 18$ OR 20

Simulated object	Actual pixels	HCM method	FCM method	CHNN method
CSF	910	910(0%)*	910(0%)	910(0%)
White matter	3698	3698(0%)	3698(0%)	3698(0%)
Gray matter	2842	2842(0%)	2842(0%)	2842(0%)
Skin/Fat	3852	3852(0%)	3852(0%)	3852(0%)
Background	26779	26779(0%)	26779(0%)	26779(0%)
Averaged error		0%	0%	0%

*The value represents the number of pixels for each simulated object, and the value in the parenthesis is the error in percentage.

TABLE II
THE SEGMENTATION PERFORMANCES FOR HCM, FCM, AND THE PROPOSED CHNN METHODS USING THE SIMULATED IMAGE WITH $K = 23$

Simulated object	Actual pixels	HCM method	FCM method	CHNN method
CSF	910	2634(189.5%)*	1224(34.5%)	893(1.8%)
White matter	3698	3734(1.0%)	4050(9.5%)	3465(6.3%)
Gray matter	2842	3720(30.9%)	4220(48.5%)	2918(2.6%)
Skin/Fat	3852	12782(231.9%)	12857(233.9%)	3946(2.4%)
Background	26779	15210(43.2%)	15729(41.3%)	26858(0.3%)
Averaged error		99.2%	73.5%	2.7%

*The value represents the number of pixels for each simulated object, and the value in the parenthesis is the error in percentage.

For the application of the medical image segmentation using the proposed algorithm of CHNN, Fig. 5(a) and (b) shows the original computed tomography (CT) images for test. Their resulting images for three classes and four classes are shown in Fig. 5(c) and (d), respectively. The MR images and their segmentation results for three regions are shown in Fig. 6. Accordingly, it is always difficult, if possible, to compare the performance of different image segmentation techniques based upon such simple measures [22]. Especially in the medical applications, different tissues may exhibit similar distribution of the gray levels. So, the quality of the segmented image usually depends heavily upon the subjective and qualitative points of view. Fig. 5 shows the CT slice in the abdomen

TABLE III
THE SEGMENTATION PERFORMANCES FOR HCM, FCM, AND THE PROPOSED CHNN METHODS USING THE SIMULATED IMAGE WITH $K = 25$

Simulated object	Actual pixels	HCM method	FCM method	CHNN method
CSF	910	2618(187.7%)*	2015(121.4%)	785(13.7%)
White matter	3698	3574(3.4%)	3709(0.3%)	3059(17.2%)
Gray matter	2842	3752(32.0%)	3996(40.6%)	3056(7.5%)
Skin/Fat	3852	13175(242.1%)	13399(247.9%)	4027(4.5%)
Background	26779	14961(44.1%)	14961(44.1%)	27153(1.4%)
Averaged error		101.9%	90.9%	8.9%

*The value represents the number of pixels for each simulated object, and the value in the parenthesis is the error in percentage.

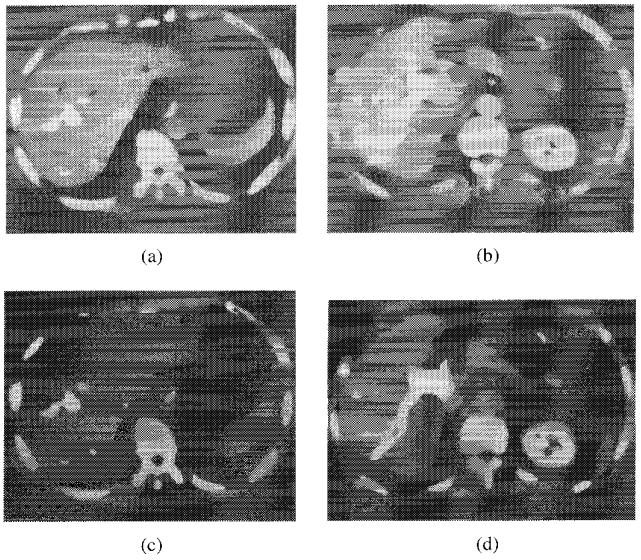

Fig. 5. (a) and (b) The original CT images, and the (c) and (d) segmented images for three classes and four classes using the CHNN, respectively.

for the diagnosis of liver disease. It is shown that the liver boundary as well as the inside portal vessels may be delineated very well. As to Fig. 6, the bone, ventricle, and gyrus regions would be reasonably segmented for further use. After all, the proposed method based upon the CHNN would segment the medical images as visually comparable to those obtained by other traditional methods [1]–[5]. It is implied that this new approach has the features of robustness to noise and initial guess. Moreover, as long as the Lyapunov energy function is used, this structure is very flexible for application in different pattern recognition problems. It is also noted that the resulting images are processed without human intervention.

In summary, from the simulation and the experiment results, the proposed algorithm could satisfactorily produce the medical image segmentation while the network convergence is guaranteed. But in fact, the Hopfield network may settle down to a local minimum after the network converges. This may be avoided by incorporating the technique of the simulated annealing into the network [23]. In the process of the medical image segmentation, the number of classes is usually known a priori from the anatomical structure. The proposed algorithm like the HCM and FCM methods would not have the problem of the determination of the class number. From the

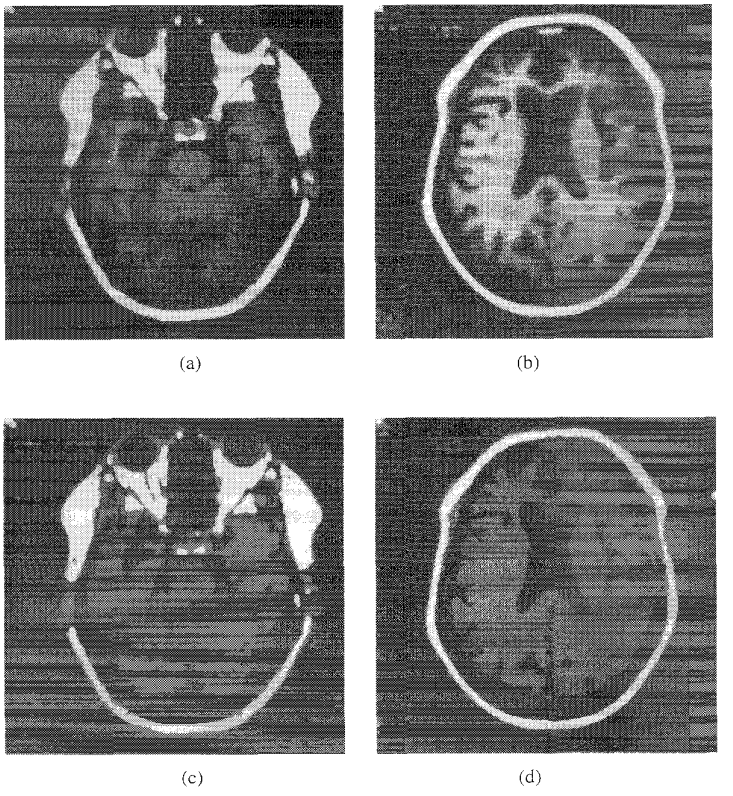

Fig. 6. (a) and (b) The original MR images and (c) and (d) the segmented images for three classes using the CHNN, respectively.

experiments, the CHNN usually takes 6–15 loops on average to be stabilized. Here, a loop is considered as the updating for all rows of the CHNN.

VI. Conclusion

In this paper, an approach using the Hopfield neural network imposed by a WTA mechanism (so-called competitive Hopfield neural network) is proposed for medical image segmentation based upon the global information of the gray levels distribution. Thus, the efforts of determining the optimal values of the weighting factors on the penalty terms may be avoided. Accordingly, the computation of this proposed algorithm can be speeded up while the convergence of network was still guaranteed. Since only the information of the global histogram but not the spatial connectivity is used in the objective function, the number of nodes in the CHNN will be independent upon the size of image. For incorporating the spatial connectivity, the segmented images may be labeled and input to another CHNN for pixel classification based upon the real distance measure between the labeled pixels and the mass centers of the classes. In this way, there is no need for changing the algorithm except for the dimension of the neurons. Certainly, the structure network may be extended to three dimension, and the computation will be more complex with the increment of the number of neurons. In addition, this proposed algorithm has great potential in parallel implementation for real-time applications.

Acknowledgment

The authors wish to thank Drs. Y.-N. Sun, P.-C. Chung, and C.-T. Tsai for their invaluable discussion, and Dr. J.-S. Lee for kindly providing the image data.

References

[1] W. K. Pratt, *Digital Image Processing.* NY: Wiley, 1991.
[2] K. S. Fu and J. K. Mu, "A survey on image segmentation," *Pattern Recog.,* vol. 13, pp. 3–16, 1983.
[3] P. K. Sahoo, S. Soltani, A. K. C. Wong, and Y. C. Chen, "A survey of thresholding techniques," *CVGIP,* vol. 41, pp. 233–260, 1988.
[4] T. Pavlidis and Y. T. Liow, "Integrating region growing and edge detection," *IEEE Trans. Pattern Anal. Machine Intel.,* vol. 12, pp. 225–233, 1990.
[5] D. P. Panda and A. Rosenfeld, "Image segmentation by pixel classification in (gray level, edge value) space," *IEEE Trans. Circuits Syst.,* vol. 22, pp. 440–450, 1975.
[6] S. Cagnoni, G. Coppini, M. Rucci, D. Caramella, and G. Valli, "Neural network segmentation of magnetic resonance spin echo images of the brain," *J. Biomed. Eng.,* vol. 15, pp. 355–362, 1993.
[7] W. C. Lin, E. C. K. Tsao, and C. T. Chen, "Constraint satisfaction neural networks for image segmentation," *Pattern Recog.,* vol. 25, pp. 679–693, 1992.
[8] M. Morrison and Y. Attikiouzel, "A probabilistic neural network based image segmentation network for magnetic resonance images," in *Proc. Conf. Neural Networks,* Baltimore, 1992, vol. 3, pp. 60–65.s
[9] W. Snyder, A. Logenthiram, P. Santago, K. Link, G. Bilbro, and S. Rajala, "Segmentation brain images using mean field annealing," in *Inform. Process. Med. Imag., Proc. 12th Int. Conf. IPMI,* Wye, UK, 1991, pp. 218–226.
[10] A. P. Dhawan and L. Arata, "Segmentation of medical images through competitive learning," *Comput. Meth. Prog. Biomed.,* vol. 40, pp. 203–215, 1993.
[11] L. O. Hall, A. M. Bensaid, L. P. Clarke, R. P. Velthuizen, M. S. Silbiger, and J. C. Bezdek, "A comparison of neural network and fuzzy clustering

techniques in segmenting magnetic resonance images of the brain," *IEEE Trans. Neural Networks,* vol. 3, pp. 672–682, 1992.
[12] M. A. Ismail and S. Z. Selim, "Fuzzy c-mean: Optimality of solutions and effective termination of the algorithm," *Pattern Recog.,* vol. 19, pp. 481–485, 1986.
[13] M. S. Kamel and S. Z. Selim, "A threshold fuzzy c-means algorithm for semi-fuzzy clustering," *Pattern Recog.,* vol. 24, pp. 825–833, 1991.
[14] L. Bobrowski and J. C. Bezdek, "C-means clustering with the l_1 and l_∞ norms," *IEEE Trans. Syst. Man. Cybern.,* vol. 21, pp. 545–554, 1991.
[15] P. Y. Yin and L. H. Chen, "A new noniterative approach for clustering," *Pattern Recog. Lett.,* vol. 15, pp. 125–133, 1994.
[16] M. E. Brandt, T. P. Bohan, L. A. Kramer, and J. M. Fletcher, "Estimation of CSF, white and gray matter volumes in hydrocephalic children using fuzzy clustering of MR images," *Computerized Med. Imag. Graph.,* vol. 18, pp. 25–34, 1994.
[17] H. J. Zimmermann, *Fuzzy Set Theory And Its Application.* Boston: Kluwer, 1991, pp. 217–240.
[18] P. C. Chung, C. T. Tsai, E. L. Chen, and Y. N. Sun, "Polygonal approximation using a competitive Hopfield neural network," *Pattern Recog.,* vol. 27, no. 11, pp. 1505–1512, 1994.
[19] C. T. Tsai, Y. N. Sun, P. C. Chung, and J. S. Lee, "Endocardial boundary detection using a neural network," *Pattern Recog.,* vol. 26, pp. 1057–1068, 1993.
[20] J. J. Hopfield and D. W. Tank, "Neural computation of decisions in optimization problems," *Biol. Cybern.,* vol. 52, pp. 141–152, 1985.
[21] J. J. Hopfield, "Neural networks and physical systems with emergent collective computational abilities," in *Proc. Nat. Acad. Sci.,* vol. 79, 1982, pp. 2554–2558.
[22] R. C. Dubes, A. K. Jain, S. G. Nadabar, and C. C. Chen, "MRF model-based algorithms for image segmentation," in *Proc. Int. Conf. Pattern Recog.,* 1990, pp. 808–814.
[23] Y. Kim, S. A. Rajala, and W. E. Snyder, "Image segmentation using an annealed Hopfield neural network," in *Proc. RNNS/IEEE Symp. Neural Informatics and Neurocomputers,* 1992, vol. 1, pp. 311–322.